In vitro development and *in vivo* application of a platinum-based electrochemical device for continuous measurements of peripheral tissue oxygen

Niall J. Finnerty *, Fiachra B. Bolger

Chemistry Department, Maynooth University, Co. Kildare, Ireland

ABSTRACT

Acute limb ischaemia is caused by compromised tissue perfusion and requires immediate attention to reduce the occurrence of secondary complications that could lead to amputation or death. To address this, we have developed a novel platinum (Pt)-based electrochemical oxygen (O_2) device for future applications in clinical monitoring of peripheral tissue ischaemia. The effect of integrating a Pt pseudo-reference electrode into the O_2 device was investigated *in vitro* with an optimum reduction potential of -0.80 V. A non-significant ($p = 0.11$) decrease in sensitivity was recorded when compared against an established Pt-based O_2 sensor operating at -0.65 V. Furthermore, a biocompatible clinical sensor (ClinOX) was designed, demonstrating excellent linearity ($R^2 = 0.99$) and sensitivity (1.41 ± 0.02 nA μM^{-1}) for O_2 detection. Significant rapid decreases in the O_2 current during *in vivo* ischaemic insults in rodent limbs were reported for Pt-Pt ($p < 0.001$) and ClinOX ($p < 0.01$) and for ClinOX ($p < 0.001$) in porcine limbs. *Ex vivo* sensocompatibility investigations identified no significant difference ($p = 0.08$) in sensitivity values over 14 days of exposure to tissue homogenate. The Pt-Pt based O_2 design demonstrated high sensitivity for tissue ischaemia detection and thus warrants future clinical investigation.

© 2017 Elsevier B.V. All rights reserved.

1. Introduction

Oxygen (O_2) is of critical importance in a myriad of physiological processes. Thus, timely and accurate monitoring techniques are essential to assist clinicians with potential lifesaving decisions. Historically, oxygenation has been monitored subjectively by clinical assessment due to the paucity of techniques to accurately evaluate precise tissue oxygen levels. Over the past 60 years, measuring and monitoring methods have been developed to quantify oxygen supply and, more recently, to continuously assess the oxygenation of blood and tissues both invasively and noninvasively [1,2]. Currently, the traditional gold standard methods of O_2 measurement performed in hospitals are pulse oximetry (PulsOx) and arterial blood gas analysis (ABG). PulsOx was developed in 1972 by Japanese engineers [3] who noted the pulsatile components of the absorbance of red and infrared light transmitted through tissue were related to arterial haemoglobin saturation [4]. However, this method is an indirect marker of tissue perfusion and functionality is lost in the absence of a pulse wave [5]. ABG machines revolutionised critical patient care following their introduction in the late 1950's [2] as blood samples could be analysed for a range of

parameters including blood gases, haemocrit, electrolytes, metabolites, and co-oximetry. However, significant drawbacks include the time lag associated with single point measurements and the deterioration of blood samples, culminating in false readings and misdiagnoses. Moreover, both methods are unsuitable for continuous real-time O_2 measurements in peripheral tissue due to their reliance on vascular factors.

No gold standard currently exists for the early diagnosis of trauma- or thrombosis-induced complications. Acute limb ischaemia (ALI), a common cause of morbidity and mortality, is defined as a restriction in blood flow to the extremities that causes a shortage of the O_2 and glucose required for cellular metabolism. ALI pathophysiologies require timely surgical intervention to restore blood perfusion to the impacted tissue. For example, acute compartment syndrome (ACS) is a very serious condition that results from increased pressure within a muscle compartment following trauma, which can lead to muscle and nerve damage and compromised blood flow unless detected early. When the intramuscular tissue pressure becomes higher than the blood pressure within capillaries, the capillaries collapse and disrupt blood flow, O_2, and nutrient delivery to nerve and muscle cells that renders them ischaemic [6–9]. Compartment syndrome is a time-critical medical emergency, in which irreversible nerve and muscle damage can occur after just six hours of increased intra-compartmental pressure. Recovery from tissue ischaemia complications is largely dependent on tissue

---

* Corresponding author.
E-mail address: niall.finnerty@mu.ie (N.J. Finnerty).

microcirculation [10] in the smallest blood vessels, including arterioles, capillaries, and venules, which are responsible for tissue oxygenation and, ultimately, tissue (and organ) health [11].

Blood perfusion is commonly assessed by non-invasive Laser Doppler Imaging (LDI), which measures blood flow through backscattering a laser beam that interacts with moving red blood cells [12,13]. While the non-invasive nature of LDI is highly desirable, it suffers from a lack of standardisation, poor temporal resolution, and can only penetrate tissue to a maximum depth of 10 mm [10]. More recently, near infrared spectroscopy (NIRS) has demonstrated excellent clinical utility that has facilitated clinical diagnoses [14–16]. NIRS utilises light waves ranging from 680 to 800 nm to measure tissue O_2 saturation by light absorption of oxygenated and deoxygenated haemoglobin [17] with increased tissue penetration up to a depth of 15 mm [5]. However, this indirect measure of tissue oxygenation with varied predictability for any clear effect magnitude or ischemic threshold has limited the clinical applicability of NIRS [18]. Furthermore, the probe has depth measurement restrictions in that superficial muscle readily absorbs the light, while deep muscles are difficult to isolate [18].

Molecular O_2 electrochemical detection was first reported by Clark approximately 60 years ago with a gold or platinum (Pt) working electrode and an Ag/AgCl reference electrode in a KCL electrolyte encased within an O_2 permeable membrane [19,20]. Over the years, Clark-type electrodes have become the gold standard for measuring levels of O_2 in tissue [21]. In fact, the aforementioned ABG machine utilises a Clark O_2 electrode. In addition the Licox® O_2 probe, which is also based on the Clark design, is the only invasive O_2 system currently approved for clinical use, particularly for cerebral O_2 monitoring [22]. The continuous real-time monitoring with the Licox® O_2 probe in traumatic brain injury patients has gained significant traction in the last decade [21,23]. Moreover, a number of recent studies have reported applications within skeletal muscle [24–26] and the feasibility of continuous tissue O_2 measurements has been demonstrated in humans following tibia fracture [27]. Hansen et al. confirmed that the level of muscle O_2 responds rapidly to ischemia and correlates with biochemical markers of muscle ischemia, including ATP and pH [25]. The Licox® O_2 probe was designed with brain monitoring as its core application and the development of a more suitable intramuscular sensor to directly measure O_2 levels would represent a key advancement in diagnosing tissue ischemia complications, such as compartment syndrome. The onset of post-trauma compartment syndrome symptoms can range from 2 h to 6 days, and delayed diagnoses could result in permanent nerve damage, contractures, or amputation, requiring extensive follow-up consultations and procedures for otherwise healthy patients. Due to the severe health implications of acute ischaemia, the development of a medical device to detect early onset in "at risk" patients by measuring muscle oxygenation following a high impact trauma would be advantageous and extremely beneficial for clinicians.

Different electrode substrates have been utilised for the electrochemical detection of O_2, including noble metals such as Pt [21,28] and Au [29,30] and carbon-based materials comprising glassy carbon [30], carbon fibre (CFE) [31,32], and carbon paste (CPE) [28,33]. CFEs are advantageous as tissue damage is minimal following in vivo implantation; however, variations in the detection of O_2 concentrations can result from electrode placement relative to blood vessels and metabolically active sites [28]. Furthermore, their fragility renders them unsuitable for clinical monitoring. On the other hand, CPEs demonstrate excellent long-term stability once implanted [33], however, there are biocompatibility concerns related to the gradual leeching of oil and paste upon contact with lipids in tissue [34]. Pt is the preferred choice of electrode substrate in the majority of electrochemical O_2 sensors due to its excellent ability to electrocatalyse the reduction of molecular O_2 through a single step, four-electron process to H_2O [21,28]. Furthermore, its biocompatibility makes it an ideal candidate for acute and chronic implantation in the human body [35]. It is a major component of many medical devices in use worldwide for assessing conditions such as heart disease, stroke, neurological disorders, and chronic pain [35]. This work describes the in vitro development of a novel and implantable Pt-based electrochemical sensor (ClinOX) for monitoring peripheral tissue O_2 using a sensing component suitable for future patient monitoring. The in vitro performance of this ClinOX design was investigated and compared against a pre-clinical Pt design. The efficacy of the different designs at measuring peripheral tissue ischaemia was investigated in small and large animal models. Finally, the effect of long-term exposure to muscle tissue homogenate on Pt sensitivity was investigated ex vivo. The work described demonstrates the feasibility of a Pt-based electrochemical device for the continuous real-time monitoring of peripheral tissue O_2 in humans in the future.

2. Materials and methods

2.1. Chemicals and solutions

All reagents used in phosphate buffered saline (PBS), i.e. sodium chloride (NaCl), sodium hydroxide (NaOH) and sodium hydrogen phosphate (NaH_2PO_4), and clinical interference studies, i.e. acetaminophen and acetylsalicyclic acid, were purchased from Sigma Aldrich Chemical Co. (Dublin, Ireland).

2.2. Electrode manufacture

The electrodes used in this study were manufactures as follows:

2.2.1. Platinum (Pt) disk working electrodes (O_2 electrode)
Pt disk electrodes were made from Teflon®-insulated Platinum/Iridium (Pt/Ir 90%/10%) wire (127 μm bare diameter, 203 μm coated diameter (5 T), Science Products GmbH, Hofheim, Germany). The electrodes were 5 cm in length and were prepared by carefully cutting 2 mm of the Teflon® insulation from one end of the wire. A gold electrical contact (in vitro: Fine Science Tools GmbH, Heidelberg, Germany; in vivo: Bilaney Consultants, Sevenoaks, UK) was soldered for rigidity to the bare end to enable connection with electrochemical instrumentation. A fresh surface was cut at the opposite end of the wire to generate an active disk surface for electrochemical reactions.

2.2.2. Pt cylinder electrodes
Pt cylinder electrodes were manufactured in a similar manner, except that a cylinder surface was prepared by removing 5 mm of the Teflon® insulation from the active end of the wire. These cylinder electrodes served as pseudo-reference electrodes (PRE) and auxiliary electrodes for Pt-Pt O_2 sensors.

2.2.3. Pt-SCE O_2 sensor
This sensor design consisted of a Pt disk O_2 electrode, a saturated calomel electrode (SCE) as the reference electrode, and a Pt rod that acted as the auxiliary electrode.

2.2.4. Pt-Pt O_2 sensor
The sensor design comprised a Pt disk O_2 electrode, a Pt cylinder PRE, and a Pt cylinder auxiliary electrode.

2.2.5. Clinical O_2 sensor (ClinOX)
The sensor was manufactured in a two-step process as represented schematically in Figure SM2. A nylon tip was constructed using injection moulding (Clada Medical Devices, Galway, Ireland). A channel was incorporated into this nylon tip to facilitate a 1–2 mm length of 500 μm bare Pt rod (Advent Research Materials, Oxford, UK). A 25 cm length of Teflon® insulated 100 μm copper wire (Goodfellow, Huntingdon, UK) was soldered to the Pt rod following removal of 2 mm Teflon® insulation at one end. This construct was then fed through the channel and the Pt rod was secured using epoxy with 0.1–0.2 mm protruding from the nylon tip and the copper wire from the opposite end. A scalpel

was used to cut a disk surface flush to the nylon tip and a smooth surface was ensured with polishing paper. Electrical contact was confirmed between the Pt disk and the exposed copper wire.

A 20 cm length of 1 mm diameter extruded biocompatible PeBax® polymer sheath (Clada Medical Devices, Galway, Ireland) was used in the construction of the sensor shaft. Briefly, two holes were created ca. 0.25 cm and 0.50 cm from one end of the sheath. Two lengths (25 cm) of Teflon® insulated copper wire, with ca. 2 mm of metal exposed at both ends, were fed through each of the pierced holes in the sheath to the opposite end with ca. 5 cm excess outside the end of the sheath. Two Pt marker bands (1.1 mm inner diameter, Fort Wayne Metals, Castlebar, Ireland) were swaged over each of the pierced holes and protruding wires, ensuring no copper wire remained exposed outside the sheath. Electrical connection was confirmed between the marker band and the respective copper wire. The copper wire was fed from the previously prepared nylon tip/wire construct down through the sheath, and the tip was glued in place at the shaft end The internal sheath cavity encompassing the marker bands and moulded nylon tip was filled with biocompatible glue (MasterBond, New Jersey, USA), to prevent fluid entry. More glue was incorporated into the junction between the marker band and sheath to prevent fluid entry, taking care not to cover the marker band.

Finally, a stress relief component was glued to the opposite sheath end with protruding lengths of exposed copper wire. The respective components of an electrical connector (Farnell Element 14, Leeds, UK or Fischer Connectors, Edinburgh, UK) were placed around this sheath end and each exposed copper wire was soldered into corresponding pins on their respective connectors. The wires were tested for electrical contact between the marker bands, Pt disk, and connector pins. Once electrical contact was confirmed, the respective connector was carefully screwed in place and electrical connection was confirmed for the final device.

2.3. In vitro calibrations

All calibrations were performed in a standard three-electrode glass electrochemical cell containing 20 mL PBS. The PBS was purged with either N_2 gas (BOC Ireland), atmospheric air (RENA air-pump) or O_2 gas (BOC Ireland) for 20 min and the appropriate gaseous atmosphere was maintained for 15 min over the cell solution during quiescent recordings. The concentrations of solution O_2 were taken as 0 μM (N_2-saturated), 240 μM (air-saturated) and 1200 μM (O_2-saturated) [28].

2.3.1. Cyclic voltammetry (CV) studies #1
Pt-SCE O_2 sensors (see Section 2.2.3) were cycled (0.20 V → −0.80 V, 100 mVsec^{-1}) in N_2, air, and O_2 saturated PBS.

2.3.2. Cyclic voltammetry (CV) studies #2
Pt-Pt O_2 sensors (see Section 2.2.4) were cycled (0.20 V → −1.0 V, 100 mVsec^{-1}) in N_2, air and O_2 saturated PBS.

2.3.3. O_2 sensor calibration #1
Pt-SCE O_2 sensors were calibrated as described above using constant potential amperometry (CPA) at −0.65 V vs. SCE.

2.3.4. O_2 sensor calibration #2 (Pt-Pt device)
Pt-Pt O_2 sensors were calibrated as described above using CPA at −0.65 V vs. Pt and −0.80 V vs. Pt.

2.3.5. O_2 sensor calibration #3 (ClinOX device)
ClinOX sensors (see Section 2.2.5) were calibrated as described above using CPA at −0.80 V vs. Pt.

2.3.6. Clinical interference studies on Pt-Pt O_2 sensor
Further interference studies were performed on Pt-Pt O_2 sensors using acetaminophen and acetylsalicylic acid. A physiologically relevant concentration (500 μM) of both interferents was added to N_2 saturated PBS and the current response was recorded over a five-minute period. The maximum current at the end of this period was compared against the pre-injection baseline level.

2.4. Open circuit potential (OCP) investigations

OCP investigations were performed in PBS using a voltmeter (Iso-Tech, Southport, UK). The voltage difference was measured between the Pt working electrode and the respective reference electrode. Furthermore, the stability of the PRE with respect to the SCE was also determined with respect to time. The voltage was recorded every 10 s over a 20-min period and the data plotted. In addition, longer term studies involved a voltage point recorded every 10 min over an 80-min period.

2.5. Ex vivo sensocompatibility calibrations

Different sets of Pt-Pt O_2 sensors were stored in homogenised porcine tissue at 4 °C for 1, 3, 7, or 14 days. The devices were then rinsed in distilled H_2O and an O_2 calibration over a 0–1200 μM concentration range was performed using CPA.

2.6. In vivo experimental and hind limb ischaemia protocol

2.6.1. Rodent experiments
Male Wistar rats (Charles River, UK, 400–600 g) were housed with a maximum of three per cage in a temperature (17–23 °C), humidity, and light controlled (12 h light, 12 h dark cycle) environment at Maynooth University. Food and water were available ad libitum. The subjects were allowed to acclimatise for at least one week prior to surgery. For in vivo experiment 1, the Pt-Pt O_2 sensors were implanted into left and right hind limbs (see Fig. 3A and SM1) through a 21G hypodermic needle. For in vivo experiment 2, ClinOX devices were implanted into left and right hind limbs through a 14G hypodermic needle. Once implanted, the hypodermic needles were retracted from the tissue. The rats were anaesthetised with Isoflurane anaesthesia (Abbott Laboratories, Dublin, Ireland) in the supine position with the anaesthesia mask fixed tightly around the nose. The subject was kept on a heating pad for the duration of the recording to prevent hypothermia. A sterilised tourniquet was placed around the subject's limb (greater trochanter) in close proximity to the body to facilitate occlusion of the blood supply. Ischaemia was induced by pulling the tourniquet as tight as possible, verified visually by the increasing pallor of the subject's foot, and was maintained for a 10-min period. Once completed, the tourniquet was removed and recordings continued for a further 20 min. Subjects were euthanised upon completion of recordings by intraperitoneal injection of Euthatal. All experimental procedures were performed at Maynooth University under license in accordance with the European Communities Regulations 2002 (Irish Statutory Instrument 165/2013).

2.6.2. Porcine experiments
Male Landrace pigs (sourced by the Biomedical Research Facility, Beaumont Hospital, Dublin, Ireland, 45–75 kg) were housed, with a maximum of four per room, in a temperature (17–23 °C), humidity, and light controlled (12 h light, 12 h dark cycle) environment at the Biomedical Research Facility, Beaumont Hospital, Dublin. Food and water were available ad libitum. The subjects were allowed to acclimatise for at least 48 h prior to surgery. For in vivo experiment 3, ClinOX devices were implanted into left and right limbs through a 14G hypodermic needle. Once implanted, the hypodermic needles were retracted from the tissue. The limb was extended and held in position for the duration of the recording using a retort stand and clamp (see Figure SM3). The pigs were anaesthetised by trained staff at the research facility using standard operating procedures and placed in the supine position for the duration of the recording. Subjects were kept under isoflurane anaesthesia throughout. A sterilised tourniquet (SP Services, Shropshire,

UK) was placed around the subject's limb in close proximity to the body to facilitate occlusion of the blood supply. Ischaemia was induced by twisting the tourniquet bar as tight as possible and fixing it into a locking mechanism. The ischaemic insult was maintained for 10 min. Once completed, the tourniquet bar was removed from the locking mechanism and loosened. The recordings continued for a further 20 min. Subjects were euthanised upon completion of recordings by trained staff at the research facility. All experimental procedures were performed at the Biomedical Research Facility, Beaumont Hospital, Dublin under license in accordance with the European Communities Regulations 2002 (Irish Statutory Instrument 165/2013).

2.7. In vivo amperometric recordings

All recordings were carried out with the subjects under general anaesthesia. For Experiment 1, all electrodes were connected *via* corresponding gold electrical contacts to a bespoke three-core cable, and soldered to contacts in a jack plug adaptor (Farnell Element 14, Leeds, UK), which was connected to the respective potentiostat (described in Section 2.8). For Experiment 2 and 3, the ClinOX device was connected *via* jack plug connection and Fischer Connector, respectively, which were then connected to their respective potentiostats (described in Section 2.8). The desired reduction potential was applied to the respective O_2 devices and the currents were allowed to stabilise for 10–15 min prior to inducing ischaemic insult. In total, each recording was performed for 45 min.

2.8. Instrumentation, software and data acquisition

In vitro CPA and CV experiments were performed using a low-noise potentiostat (ACM Instruments, Cumbria, UK) and converted using an A/D converter (PowerLab, ADInstruments, Oxford, UK) running on a Dell computer. The CPA and CV signals were recorded using LabChart software (v8, ADInstruments, Oxford, UK) and eChem software (v2.1.16, eDAQ Ltd., Sydney, Australia), respectively. All data analysis was performed using GraphPad Prism v5 (GraphPad Software Inc., San Diego, CA, USA).

For *in vivo* experiments 1 and 2, the amperometric O_2 current was detected using a prototype single channel potentiostat (Bluebridge Technologies, Dublin, Ireland) and converted using an A/D converter (PowerLab). The digital signal was then recorded using LabChart software v8 running on a Dell Laptop. All data analysis was performed using GraphPad Prism v5. For *in vivo* experiment 3, the amperometric O_2 current was detected using a rechargeable battery-operated single channel potentiostat with an in-built A/D converter (Bluebridge Technologies, Dublin, Ireland). This clinically viable hardware unit provides the added benefit of removing the direct electrical contact between device and patient, significantly increasing benefit-to-risk rationale. This potentiostat is ISO 13485 compliant and is a battery-operated version of the prototype utilised during *in vivo* experiments 1 and 2 (see Figure SM5) with telemetric functionality. The digital signal was recorded using a custom designed IEC 62304 compliant IOS App (Bluebridge Technologies, Dublin, Ireland) running on an Apple iPad (see Figure SM5). All data was compiled in Microsoft Excel and all data analysis was performed using GraphPad Prism v5 (GraphPad Software Inc., CA, USA).

All *in vivo* figures presented had baseline levels normalised to 100% to illustrate the overall change in current as a % of the pre-ischemia baseline level. This removes both inter-electrode and inter-animal variability by ensuring that the presented current changes are representative of the data from all animals used in each study. Reported *in vivo* concentration changes are based on *in vitro* pre-calibration curves, *i.e.* average slope/sensitivity recorded for respective O_2 sensor designs. For clarity, all *in vivo* currents have been transformed to positive values. For *in vitro* and *in vivo* investigations, significant differences were calculated using the Student's *t*-test for paired or unpaired observations,

where appropriate. For *ex vivo* sensocompatability investigations, the significant differences observed were calculated using one-way ANOVAs with a Bonferroni post-hoc test. Two-tailed levels of significance were set at $p < 0.05$. *n* values are representative of the number of ischaemic insults/number of animals.

3. Results

3.1. In vitro investigations comparing Pt-Pt and Pt-SCE electrochemical designs

Fig. 1A and B show the CV investigations of the O_2 reduction characteristics of Pt-Pt and Pt-SCE designs in air and O_2 saturated PBS. It should be noted that the potential window for the Pt-SCE design was restricted to -0.80 V to mitigate interference from the generation of H_2, which is initiated at this potential. It is apparent from the voltammograms that the maximum currents for both Pt designs are comparable; however, the reductive peak is pushed to a more negative potential and more defined, albeit broader, in the Pt-Pt design. The foot of the reductive wave for the Pt-SCE in both air-saturated and O_2-saturated PBS commenced at -0.20 V and the maximum peak between -0.25 V and -0.30 V, which is comparable to that reported previously for the same design [28]. In contrast, the reductive foot for the Pt-Pt design commenced at -0.40 V for both O_2 concentrations, while the reductive peak occurred at -0.55 V in air-saturated and -0.60 V in O_2-saturated PBS. A more negative potential infers that discrete equilibrium potentials exist between working and reference electrodes in both configurations. This was confirmed by OCP measurements performed between the Pt working electrodes and the respective reference electrodes, *i.e.* SCE and PRE. Fig. 1C illustrates the OCP measured between the Pt electrode and SCE over a 20-min period. The OCP measured at 20 min (0.22 V) demonstrated a slight drift over this period, but the potential stabilised (see Fig. 1C inset) when investigated over a longer 80-min period. A similar trend was observed in the OCP measured between the Pt electrode and PRE, albeit at a lower potential (0.09 V). A slight drift in OCP was recorded over a 20-min period (Fig. 1D), but this stabilised towards the end of the 80-min recording. The difference in OCP (Δ 0.13 V) between configurations lends support to the variations observed between reduction waves in Fig. 1A and B. Furthermore, when OCP measurements were undertaken with PRE *vs.* SCE, a voltage difference of 0.21 V was identified after 20 min. A similar trend in voltage drift is clearly evident in Fig. 1E, thus supporting a stable drift in equilibrium potential between both configurations.

It was therefore decided to apply the previously published -0.65 V reduction potential [28] and a more negative -0.80 V reduction potential to the Pt-Pt configuration for subsequent CPA investigations. A maximum potential of -0.80 V *vs.* Pt was chosen to alleviate concerns surrounding the unfavourable generation of H_2 *in vivo*, which occurs through the electrolysis of water at potentials close to -0.80 V *vs.* SCE (data not shown). An initial O_2 calibration over the concentration range 0–1200 μM was performed on the Pt-SCE design at -0.65 V *vs.* SCE, which demonstrated excellent linearity ($R^2 = 0.99$) and good sensitivity (0.79 ± 0.07 nA μM^{-1}, $n = 8$, Table 1). However, an O_2 calibration on the Pt-Pt design at -0.65 V *vs.* Pt demonstrated a significantly reduced ($p < 0.001$) sensitivity (0.37 ± 0.05 nA μM^{-1}, $n = 8$) and linearity ($R^2 = 0.98$). This was not entirely unexpected based on the voltammograms presented in Fig. 1A and B. The larger negative potential of -0.80 V *vs.* Pt was applied to the Pt-Pt electrode configuration and an improvement in sensitivity (0.64 ± 0.06 nA μM^{-1}, $n = 8$, Table 1) and linearity ($R^2 = 0.99$) was recorded. This increased sensitivity was significantly different ($p < 0.01$) when compared to Pt-Pt at -0.65 V *vs.* Pt, but there was no significant difference ($p = 0.11$) when compared against the Pt-SCE design at -0.65 V *vs.* SCE (see Fig. 2A and B). Furthermore, the limit of detection (LOD) was comparable across all design configurations: -0.65 V *vs.* SCE, 0.23 ± 0.04 μM ($n = 8$); -0.65 V *vs.* Pt, 0.26 ± 0.08 μM ($n = 8$); -0.80 V *vs.* Pt, 0.30 ± 0.02 μM ($n = 8$). Table 1 compares the respective *in vitro* characteristics of these
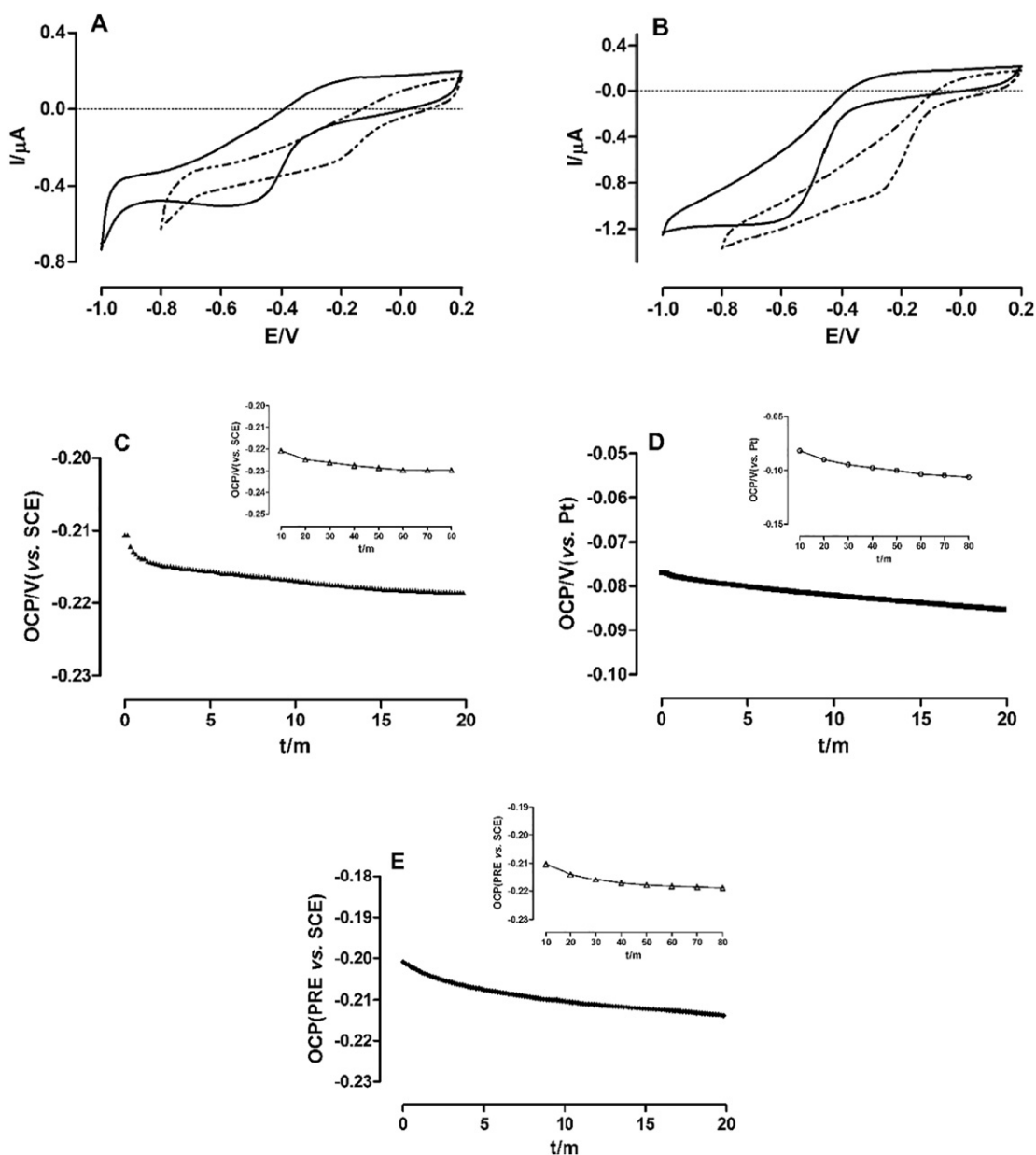
Fig. 1. Cyclic voltammetry (CV) plots comparing platinum platinum (Pt-Pt) O_2 sensor (solid line) and Pt-saturated calomel electrode (Pt-SCE) O_2 sensor (dashed line) in (A) air saturated and (B) oxygen (O_2) saturated phosphate buffered saline (PBS). 20-min open circuit potential (OCP) measurements performed on (C) Pt-SCE, (D) Pt-Pt and (E) pseudo reference electrode (PRE) *vs.* SCE in PBS. *Insets*: OCP stability measurement performed over an 80-min period.

configurations. To confirm that both Pt-SCE at −0.65 V and Pt-Pt at −0.80 V configurations demonstrate comparable signal stability, amperometric currents were recorded overnight for both configurations under ambient air conditions (21% O_2). It is apparent from Fig. 2C that

both signals (Pt-SCE, black trace and Pt-Pt, blue trace) stabilised with respect to time, thus corroborating OCP measurements illustrated in Fig. 1C-E. Taken collectively, these findings confirm that applying −0.80 V to the various Pt-Pt configurations maximises O_2 detection.

Table 1
Summary of *in vitro* performance of various Pt-Pt amperometric O_2 devices.

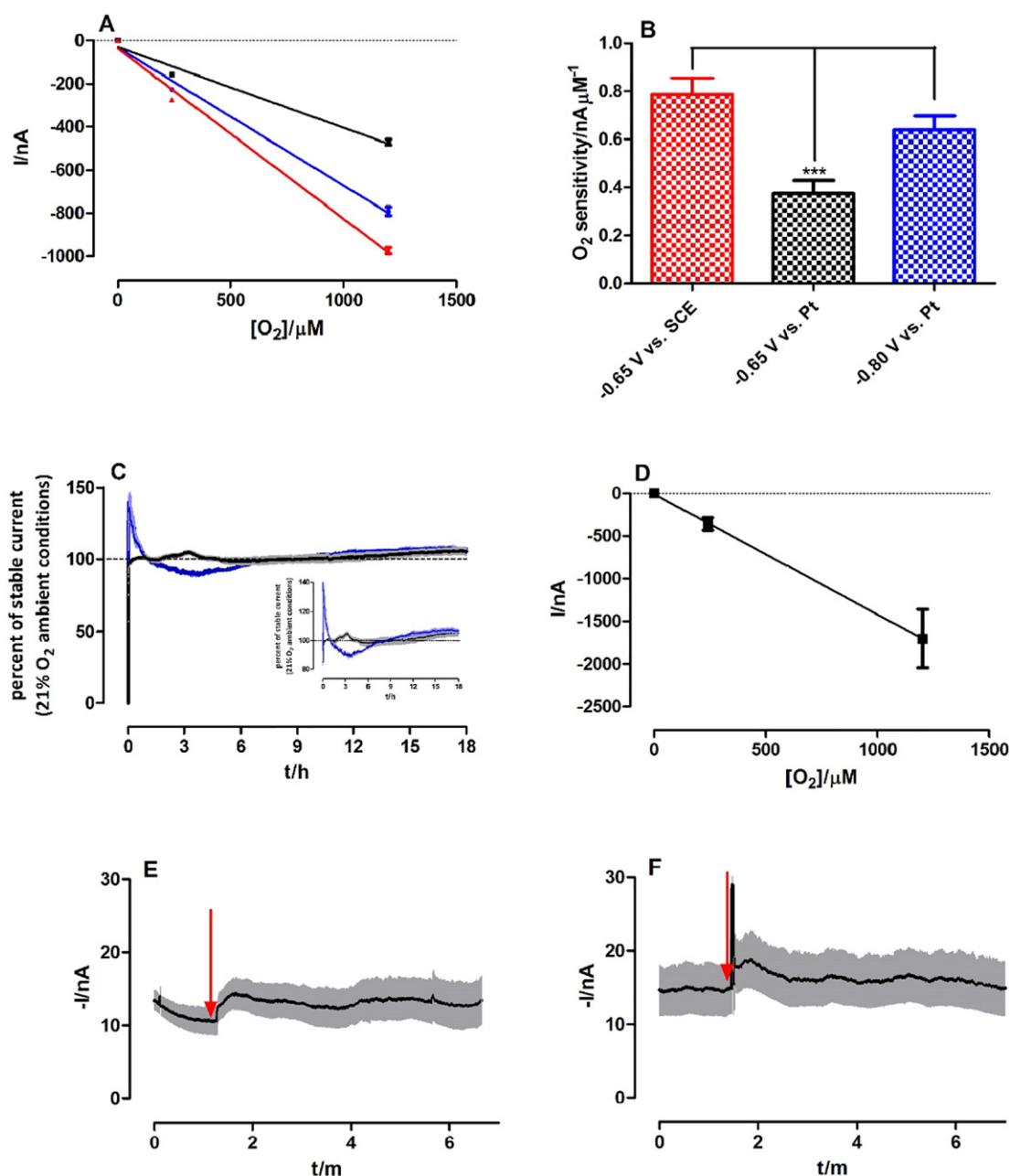|	Sensitivity (nAμM^{-1})	Current density (nA mm^{-2} μM^{-1})	Limit of detection (LOD, μM)	Linearity (R^2)
Pt-SCE (−0.65 V *vs.* SCE) ($n = 8$)	0.79 ± 0.07	62.2 ± 5.3	0.23 ± 0.04	0.99
Pt-Pt (−0.65 V *vs.* Pt) ($n = 8$)	0.37 ± 0.05	29.5 ± 4.3	0.26 ± 0.08	0.98
Pt-Pt (−0.80 V *vs.* Pt) ($n = 8$)	0.64 ± 0.06	50.4 ± 4.6	0.30 ± 0.02	0.99
ClinOX (−0.80 V *vs.* Pt) ($n = 10$)	1.41 ± 0.02	7.2 ± 0.1	0.19 ± 0.06	0.99

Fig. 2. (A) Current-concentration profiles ($n = 8$) for (0–1200 μM) O_2 calibration on Pt-Pt O_2 sensor at -0.65 V (black trace) and -0.80 V (blue trace) and Pt-SCE O_2 sensor (red trace) at -0.65 V. (B) O_2 sensitivity comparisons for Pt-Pt O_2 sensor at -0.65 V (black column) and -0.80 V (blue column) and Pt-SCE O_2 sensor (red column) at -0.65 V. Data presented as nAμM^{-1} $\pm$ SEM ($n = 8$). * denotes level of significance. (C) Stability of amperometric current ($n = 4$) overnight for Pt-SCE at -0.65 V (black trace) and Pt-Pt at -0.80 V (blue trace) in ambient air (21% O_2) conditions (*Inset*: stability traces with shortened y axis scale). (D) Current-concentration profile ($n = 10$) for 0–1200 μM O_2 calibration on ClinOX O_2 sensor at -0.80 V *vs*. Pt. Average current response ($n = 4$) of Pt-Pt O_2 sensor to addition of (E) 500 μM aliquot of acetylsalicyclic acid and (F) 500 μM aliquot of acetaminophen to N_2 saturated PBS at -0.80 V *vs*. Pt. Mean current response represented by black trace, % error represented by grey trace.

Pt-Pt O_2 sensors were subsequently tested against acetaminophen and acetylsalicyclic acid—two electroactive interferents with a high probability of being present in patient tissue. Calibrations were performed at -0.80 V *vs*. Pt by adding 500 μM aliquots of interferent to N_2-saturated PBS and the current response recorded over a five-minute period. An initial increase in current response was observed following the addition of the respective interferents (Fig. 2E and F), but the effect was transient and the current response returned to pre-injections levels within the five-minute period. Specifically, non-significant current changes (1.75 ± 0.87 nA, $n = 4$, $p = 0.14$ and 0.29 ± 0.31 nA, $n = 4$, $p = 0.41$) were recorded for acetylsalicyclic acid and acetaminophen, respectively, compared to pre-injection levels. When comparing

these currents against the O_2 currents detected at the Pt-Pt O_2 sensors, these deviations from baseline levels were deemed negligible and likely attributed to a convective artefact associated with the addition of the respective aliquot.

3.2. In vitro comparison of Pt-Pt and novel ClinOX electrochemical designs

A novel electrochemical device suitable for clinical monitoring was designed based on feedback received from clinical experts. A single implantable device incorporating three Pt electrodes was constructed as illustrated in Figure SM2 and described in Section 2.2.5. *In vitro* calibrations performed on this novel ClinOX sensor (see Fig. 2D) over

a 0–1200 µM O_2 concentration range demonstrated excellent linearity ($R^2 = 0.99$) and sensitivity (1.41 ± 0.02 nA µM^{-1}, $n = 10$). For direct sensitivity comparisons between the ClinOX sensor and the Pt-Pt sensor, current densities were calculated to account for the different physical dimensions of the recording surface areas using the formula,

$$J = I/A$$

where 'J' refers to the current density of the disk electrode, 'I' refers to the current in nA, and 'A' refers the area of the disk electrode in mm^2. The sensitivity of the Pt-Pt device was approximately seven times that of the ClinOX device: 50.4 ± 4.6 nA mm^{-2} µM^{-1}, $n = 8$, $R^2 = 0.99$ vs. 7.2 ± 0.01 nA mm^{-2} µM^{-1}, $n = 10$, $R^2 = 0.99$, respectively (Table 1). Regardless of this discrepancy, the sensitivity of the ClinOX sensor was more than adequate for physiological measurements. In addition, the LOD was determined to be 0.19 ± 0.06 µM ($n = 10$), which was an improvement on all Pt-Pt devices described in Section 3.1.

3.3. In vivo experiment #1 – measurement of peripheral tissue O_2 current using the Pt-Pt device during acute limb ischaemia in anaesthetised rats

Amperometric O_2 currents were recorded from the hind limb of anaesthetised Wistar rats using the experimental set-up illustrated in Fig. 3A and SM1. The current was allowed to dissipate over a 10–15 min period prior to application of the tourniquet, as this time was suitable (see SM4) for establishing a stable baseline. As illustrated in Fig. 3B and Table 2, the O_2 current decreased significantly ($p < 0.001$, see Fig. 3C) by 50.6 ± 5.3 nA ($n = 12/6$) from a pre-insult baseline

level of 90.2 ± 7.3 nA following application of a tourniquet to the hind limb. The maximum response of the ischaemic insult after 4.6 ± 0.6 min corresponded to a percentage change of 59.1 ± 4.6 from pre-insult levels. Furthermore, this current change translated into a decrease in concentration of 79.0 ± 8.3 µM. The O_2 current increased immediately upon removal of the tourniquet and reperfusion levels reached a maximum (123.1 ± 10.0 nA) after 4.8 ± 0.7 min, which was significantly different from the pre-insult baseline ($p < 0.001$).

3.4. In vivo experiment #2 – measurement of peripheral tissue O_2 current using the ClinOX device during acute limb ischaemia in anaesthetised rats

The ClinOX device was implanted through a 14 G needle into the hind limb of anaesthetised rats using an identical set-up to that detailed in Figs. 3A and SM3. As previously described, the current was allowed to dissipate over a 10–15 min period prior to application of the tourniquet. Fig. 4A and Table 2 illustrate the effect of the ischaemic insult on the ClinOX device. Briefly, the O_2 current decreased significantly ($p < 0.01$, see Fig. 4B) by 105.6 ± 20.1 nA ($n = 9/6$) from a pre-insult baseline level of 166.5 ± 21.3 nA following application of the tourniquet. The maximum response of the ischaemic insult after 4.3 ± 1.1 min corresponded to a percentage change of 62.8 ± 6.5 from pre-insult levels. Furthermore, this current change translated into a decrease in concentration of 74.9 ± 14.2 µM. The O_2 current increased immediately upon removal of the tourniquet and reperfusion levels reached a maximum (154.6 ± 27.3 nA) after 5.6 ± 1.5 min. However, reperfusion levels failed to overshoot pre-insult baseline levels ($p = 0.51$).
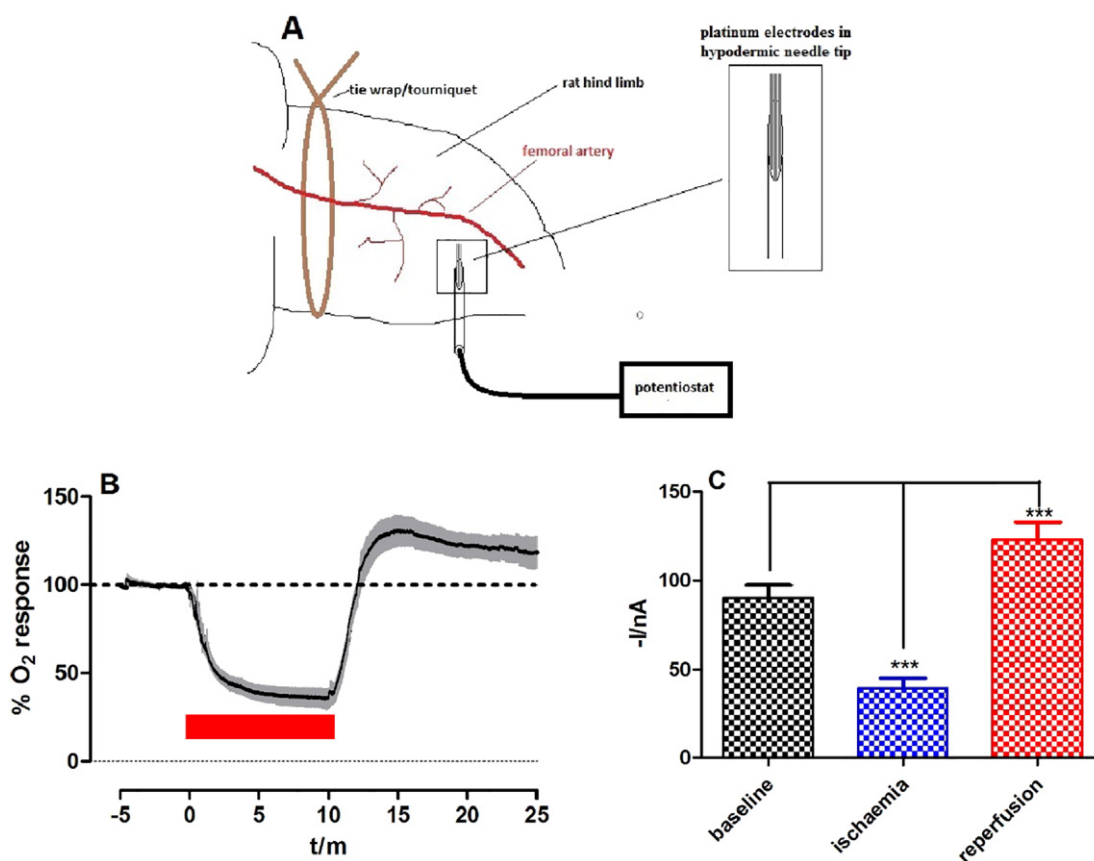

Fig. 3. (A) Schematic illustrating *in vivo* experimental set-up for continuous electrochemical detection of tissue O_2 in the rat hind limb ischaemia model. A tourniquet (tie wrap) was placed loosely around the top of the limb (greater trochanter) prior to insertion of a 21G hypodermic needle containing the Pt-Pt O_2 sensor configuration. Needle is retracted and electrode tips are left implanted in tissue. All three electrodes are connected to a potentiostat for data acquisition. (B) Average % O_2 response ($n = 12/6$) Pt-Pt O_2 sensor to a 10-min ischemic insult and subsequent reperfusion in the hind limb of an anaesthetised rat. Mean % O_2 response represented by black trace, % error represented by grey trace. (C) Comparisons of average baseline current *vs.* average ischaemic current ($p < 0.001$) *vs.* average reperfusion current ($p < 0.001$). Data represented as mean current $\pm$ SEM. * denotes level of significance.

Table 2
Summary of *in vivo* amperometric O_2 data recorded from both Pt-Pt configurations in rodent and porcine models of acute limb ischaemia.

	Baseline (nA)	Δ I (nA)	Max % response	Max I (min)	Reperfusion I (nA)	Reperfusion (min)
Pt-Pt (rat, n = 12/6)	90.2 ± 7.3	50.6 ± 5.3	59.1 ± 4.6	4.6 ± 0.6	123.1 ± 10.0	4.8 ± 0.7
ClinOX (rat, n = 9/6)	166.5 ± 21.3	105.6 ± 20.1	62.8 ± 6.5	4.3 ± 1.1	154.6 ± 27.3	5.6 ± 1.5
ClinOX (pig, n = 11/6)	128.2 ± 10.8	69.8 ± 10.2	52.5 ± 4.2	3.3 ± 0.9	145.0 ± 20.8	4.9 ± 1.4

Where 'I' denotes current.

3.5. In vivo experiment #3 – measurement of peripheral tissue O_2 current during limb ischaemia in anaesthetised pigs

The ClinOX device was implanted through a 14 G needle into the limb of anaesthetised pigs, as illustrated in Figure SM3. Similar to previous investigations, the current was allowed to dissipate over a 10-min period prior to tourniquet application. Fig. 5A and Table 2 illustrate

the effect of the ischaemic insult on the ClinOX device. In summary, the O_2 current decreased significantly ($p < 0.001$, see Fig. 5B) by 69.8 ± 10.2 nA ($n = 11/6$) from a pre-insult baseline level of 128.2 ± 10.8 nA following application of the tourniquet to the hind limb. The maximum response of the ischaemic insult after 3.3 ± 0.9 min corresponded to a percentage change of 52.5 ± 4.2 from pre-insult levels. Furthermore, this current change translated into a decrease in concentration of 49.5 ± 7.2 μM. The O_2 current increased immediately upon removal of the tourniquet and reperfusion levels reached a maximum (145.0 ± 20.8 nA) after 4.9 ± 1.4 min. However, an overshoot in
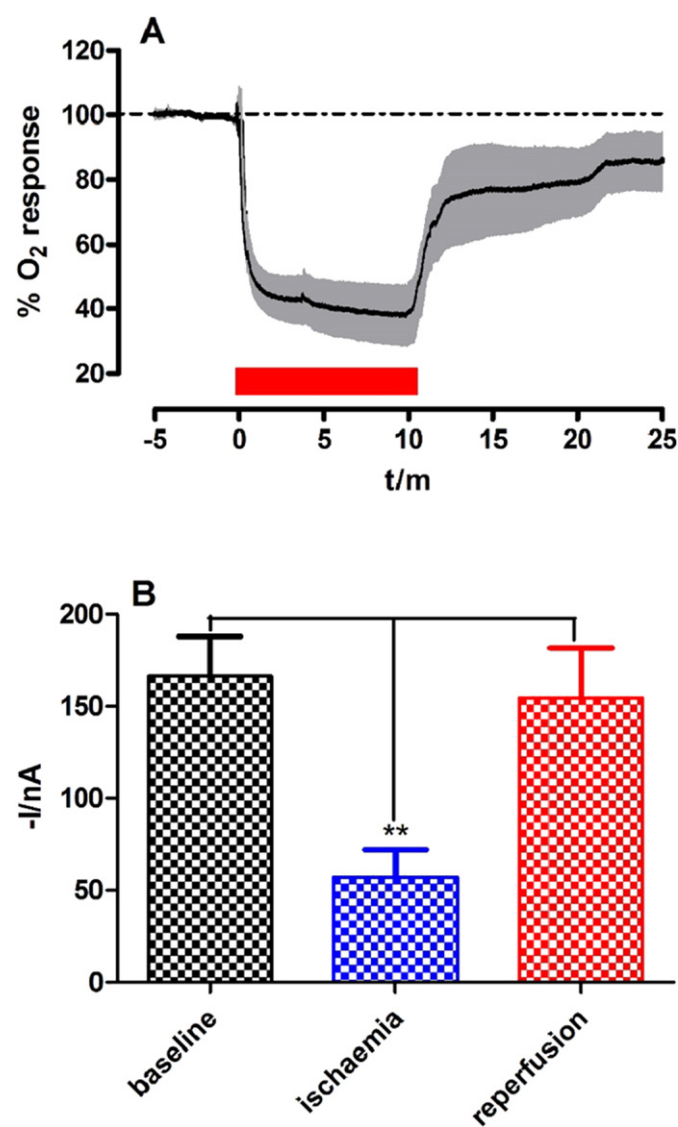

Fig. 4. (A) Average % O_2 response ($n = 9/6$) from ClinOX O_2 sensor to a 10-min ischemic insult and subsequent reperfusion in the hind limb of an anaesthetised rat. Mean % O_2 response represented by black trace, % error represented by grey trace. (B) Comparisons of average baseline current *vs.* average ischaemic current ($p < 0.01$) *vs.* average reperfusion current ($p = 0.51$). Data represented as mean current ± SEM. * denotes level of significance.
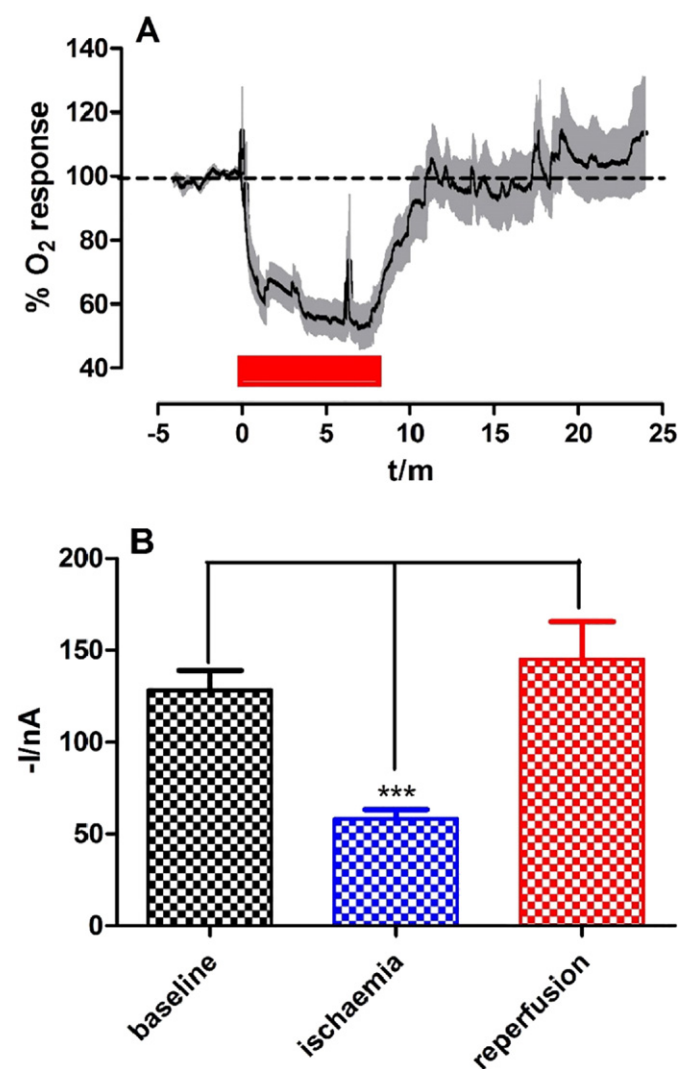
Fig. 5. (A) Average % O_2 response ($n = 11/6$) ClinOX O_2 sensor to a 10-min ischemic insult and subsequent reperfusion in the hind limb of an anaesthetised pig. Mean % O_2 response represented by black trace, % error represented by grey trace. (B) Comparisons of average baseline current *vs.* average ischaemic current ($p < 0.001$) *vs.* average reperfusion current ($p = 0.38$). Data represented as mean current ± SEM. * denotes level of significance.

current was absent and the current returned back to similar to pre-insult baseline levels ($p = 0.69$).

3.6. Ex vivo sensocompatibility studies on Pt-Pt design

The interaction that results from sensor implantation into tissue is one of the major obstacles for developing viable long-term implantable sensors. All implanted devices are subject to physiological responses, including protein and lipid adsorption. Therefore, it was decided to investigate the effect of long-term exposure (Day 1–14) of porcine tissue homogenate on the sensitivity of the Pt-Pt design ex vivo. It is evident from Fig. 6 that there is a negligible effect of the tissue homogenate over a 14-day period when compared to non-treated Pt-Pt devices. In summary, the sensitivities recorded on Day 0 (0.64 ± 0.06 nA µM^{-1}, n = 8, R^2 = 0.99), Day 1 (0.38 ± 0.06 nA µM^{-1}, n = 4, R^2 = 0.98), Day 3 (0.49 ± 0.10 nA µM^{-1}, n = 4, R^2 = 0.99), Day 7 (0.40 ± 0.08 nA µM^{-1}, n = 4, R^2 = 0.97) and Day 14 (0.45 ± 0.06 nA µM^{-1}, n = 4, R^2 = 0.99) demonstrated no significant difference ($p = 0.08$, one-way ANOVA), which suggested retained stability following tissue exposure. Bonferroni post-hoc analysis identified no significant variation in sensitivities across Day 1 and Day 14 ($p = 0.84$), which is more representative of the actual effect of tissue exposure on sensor performance given that there was no exposure to tissue homogenate on Day 0. This assumption was supported further by unpaired t-tests performed between individual exposure days. A significant decrease in sensitivity ($p = 0.03$) was recorded initially between Day 0 vs. Day 1, which corroborates previous reports using implantable brain sensors [36,37]. However, there were no further significant differences between Day 1 vs. Day 3 ($p = 0.54$), Day 1 vs. Day 7 ($p = 0.95$), or Day 1 vs. Day 14 ($p = 0.69$). This demonstrates the in vivo stability of the Pt-Pt device over a 14-day exposure period, thus supporting its potential utility for continuous long-term clinical monitoring.

4. Discussion

Many microelectrode types have been used for the electrochemical reduction of molecular O$_2$ [28,33,37,38]. Platinum has particularly excellent electrocatalytic properties that make it an ideal candidate for O$_2$ reduction [21], which consists of a four-electron reduction to H$_2$O:

$$O_2 + 4H^+ + 4e^- \rightarrow 2\,H_2O$$
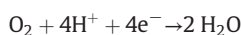
Previous work has demonstrated excellent in vitro characteristics for Pt-based electrodes, including high sensitivity, interference free signals, no pH or ion effects, as well as comparable detection limits and response times to CPEs [28]. For in vivo recordings, the conventional reference electrode is typically replaced by a miniature PRE. Therefore, it was imperative to investigate the effect of changing reference electrodes on the O$_2$ reduction potential using cyclic voltammetry. The essential difference between SCE and PRE reference electrodes is a poorly defined equilibrium potential in PREs between the metal and solution phase [39], thus making it difficult to calculate the exact potential of PREs. However, Ag-PRE electrodes have demonstrated excellent stability in vivo following long-term implantation in the brain of freely moving rats [40–42] and mice [43]. For our purpose, we chose a Pt-PRE due to its aforementioned inert biocompatible characteristics. Figs. 1A and B illustrate a shift in reduction potential to a more negative value, most likely explained by discrepancies in the equilibrium potential between the Pt electrode and the respective reference electrodes. This was substantiated through OCP measurements performed with respect to both electrode configurations. OCP measurements identified an equilibrium potential variance of 0.13 V between configurations, which may explain the difference in reductive wave potentials observed in Figs. 1A and B. In addition, OCP investigations illustrate a slight drift in potential with respect to dissipation times in both configurations after ca. 60 min, although greater stabilisation was observed with the Pt-SCE design. In fact, the overall drift in equilibrium potential in the Pt-Pt design stabilises with time and would not translate into unpredictable O$_2$ current drifts, further supporting the reliability of use in long-term recordings. This was substantiated by OCP measurements performed between PRE vs. SCE. Furthermore, when the amperometric O$_2$ current was investigated in PBS exposed to ambient air (21% O$_2$), both Pt-SCE (at −0.65 V) and Pt-Pt (at −0.80 V) configurations demonstrated equivalent signal stability over an 18-h period. Collectively, these findings illustrate the comparable performances of both electrode configurations, thus alleviating concerns regarding PRE incorporation into the design.

The previously reported −0.65 V and experimentally identified −0.80 V were both applied to the Pt-Pt design during CPA experiments. A significant difference in sensitivity was recorded between both potentials, but no significant differences were observed when sensitivities of the Pt-SCE design at −0.65 V vs. SCE and Pt-Pt design at −0.80 V were compared. This lends support to the latter being the optimal potential for maximising O$_2$ detection using the miniaturised Pt-Pt design. Further, in vitro investigations were performed on our novel ClinOX design to evaluate its performance characteristics over the conventional O$_2$ calibration range and larger reduction potential with clinical monitoring as a target application. In the field of medical devices, platinum's durability, inertness, and electrical conductivity make it the ideal electrode material for devices ranging from pacemakers, implantable defibrillators, neuromodulation devices, and cochlear implants [35]. The ClinOX device demonstrated excellent linearity and improved sensitivity on the Pt-Pt design. Table 1 compares the analytical performance of the respective Pt-Pt and Pt-SCE configurations in terms of key in vitro parameters, such as LOD, linearity, and current density (J). The latter permits a sensitivity comparison across varying electrode geometries. Despite the large disparity between J values, the sensitivity and improved LOD calculated for the ClinOX device make it more than adequate for in vivo monitoring. Similar current densities and LODs have been reported previously by other groups for the electrochemical detection of O$_2$ on Pt substrates [21,28]. The selectivity of Pt electrodes for O$_2$ reduction has been demonstrated previously against a myriad of electroactive interferents found in brain ECF with <1% contribution to the overall signal detected at 50 µM O$_2$ [28]. The majority of these interferents are also present in peripheral tissue where O$_2$
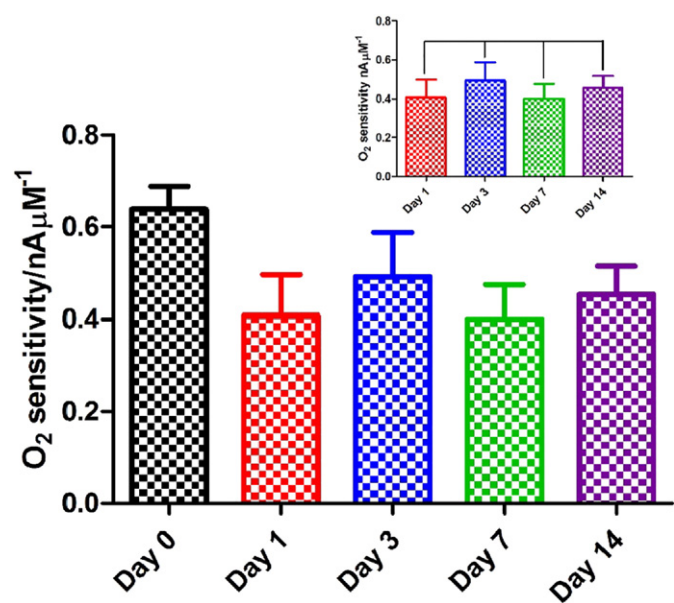

Fig. 6. Pt-Pt sensitivity values recorded at −0.80 V vs. Pt over 0–1200 µM concentration range following long-term exposure (0–14 days) to porcine tissue homogenate. Inset: Day 1–14 porcine tissue statistical analysis. Data presented as nAµM^{-1} ± SEM.

concentrations are expected to be higher than brain levels [28]. In addition, due to the clinical focus of this work, further investigations were undertaken against acetaminophen (paracetamol) and acetylsalicylic acid (aspirin), both of which are likely to be present in patient interstitial fluid. Negligible interference was observed for both electroactive species, even at an O_2 concentration of 0 μM. The absence of O_2 signal interference can be attributed in part to the large faradaic currents generated as a result of O_2 detection that mitigate against a myriad of potential sources of interference.

The efficacy of the Pt-Pt design in measuring O_2 changes within skeletal tissue was subsequently examined by implanting both Pt-Pt configuration (Pt-Pt and ClinOX) designs in peripheral tissue and exposing the limb to acute ischaemia under tourniquet control. Tourniquets are routinely clinically applied to maintain a bloodless field during surgeries in the area of the limb distal to the occlusion. Rendering the limb of an animal ischaemic is currently considered to be the most effective method for simulating the conditions of haemodynamic complications, including critical limb ischaemia and compartment syndrome [44]. The rodent is most frequently utilised with surgical procedures ranging from arterial ligation [44,45], complete excision [46,47], electrocoagulation [46], and the application of a tourniquet around the limb [48]. Furthermore, since the targeted application for the ClinOX device was clinical monitoring, the larger porcine model was also investigated since it more closely represents the size and haemodynamics of the human vascular system [44]. Table 2 provides a summary of the *in vivo* amperometric O_2 data recorded from both Pt-Pt configurations in rodent and porcine models of acute limb ischaemia. Both Pt-Pt configurations recorded immediate and significant decreases (*ca.* 50–60%) in amperometric currents that demonstrated similarities across subjects when normalised values were calculated. Since the amperometric O_2 current measured at the sensor surface is a balance between the O_2 supplied from the vasculature and that utilised by the surrounding tissue [49], we postulate that the decrease in current is attributed to a reduced blood O_2 supply following tourniquet application, while cellular utilisation remains constant throughout the ischemic insult. This would result in a net decrease in the O_2 current. Furthermore, there was no significant variation in the maximum response times ($p = 0.58$, one-way ANOVA, $n = 6$), indicating that a comparable level of ischaemia was induced followed tourniquet application across all Pt-Pt configurations and animal species investigated. These findings corroborate recent work using non-invasive imaging in porcine limb that measured an immediate drop in oxygenated haemoglobin (within the first 10 min) after induction of ischaemia that continued to decrease over the course of the insult (3–4 h), albeit at a much slower rate [10]. Their objective was to measure locomotion recovery and required significantly longer durations of ischaemia to achieve this. The principle objective of our work was to demonstrate the feasibility of a novel Pt-Pt electrode configuration for measuring tissue O_2 changes during an ischaemic episode and, as such, the insult duration was of little significance. Nevertheless, there are striking similarities between both configurations that strongly support the validity of our device at measuring tissue perfusion. Other work reported that ischaemic insult causes a decrease in glucose concentration and a concurrent increase in lactate concentration, measured using microdialysis [48]. The increase in lactate postulates anaerobic glycolysis in the absence of O_2 availability—a finding that was attenuated following exposure to hyperbaric O_2.

Reperfusion following tourniquet release produced variable responses across Pt-Pt configurations and animal species. The Pt-Pt design (Fig. 3B and C) resulted in a significant ($p < 0.001$) overshoot in the reduction current following cessation of ischaemia, which corroborates work described by others [10,48]. Conversely, the ClinOX device (Fig. 4A and B) showed an immediate increase in O_2 current upon tourniquet removal, but no overshoot was observed ($p = 0.51$) when compared to pre-insult level in the rodent hind limbs. A plausible explantation for this could be that the form factor of the larger ClinOX device renders it unsuitable for measurements in rodent limbs since a significant

overshoot was reported in the identical animal model using the smaller Pt-Pt design. It is apparent from Fig. 4A that the reduction current gradually returned to pre-insult levels during reperfusion. However, the diffusion of the analyte to the electrode surface may be hindered by the geometry or tubular design of the ClinOX device. This hypothesis was somewhat substantiated during reperfusion recordings in the porcine model. It is apparent from Fig. 5A that although an overshoot was not apparent ($p = 0.38$), the reduction current quickly returned to pre-insult levels and stabilised. Albeit variable, the reperfusion response recorded across all Pt-Pt configurations clearly illustrated an immediate increase in current during the restoration of blood flow. Intuitively, this suggests that the reduction current is increasing due to an increase in the O_2 supply from the vasculature upon removal of the tourniquet. The overshoot in current observed from the Pt-Pt design in rat limb recordings is in line with previous work [10] that reports an overshoot in oxygenated haemoglobin compared to pre-ischaemic levels. The transient nature of this overshoot is identical to that observed in Fig. 3B. This can possibly be explained by an increase in tissue O_2 utilisation following the ischaemic episode that eventually returned the current to stable levels representative of a balanced O_2 supply and utilisation.

Sensocompatibility investigations were performed *ex vivo* whereby the complete Pt-Pt design of the O_2 electrode, PRE, and auxiliary electrode were exposed to homogenised porcine muscle tissue for a specified duration. Sensocompatibility is a term coined by Wisniewski and colleagues to describe the effect the body has on an electrochemical sensor [50], and has been reported previously for different sensors [28,51]. The *in vivo* environment presents a complex chemical milieu that includes electrode contaminations, such as lipids, proteins, and a tissue matrix that restricts mass transport to the electrode surface and physiologically reacts to a sensor's presence [36,37,52]. The effect of brain homogenate on Pt electrodes has been reported previously whereby bare Pt electrodes demonstrated a decrease in sensitivity after three days of exposure, though no significant difference was noted when compared against non-treated electrodes [28]. In our case, a drop in sensitivity after 24 h of exposure was noted, which illustrated a negligible deviation over the subsequent 14 days. This initial compromise in sensitivity is to be expected following tissue homogenate contact [37]. The adhesion and proliferation of fouling agents such as proteins and lipids on all Pt electrodes serve to briefly degrade the device's functionality. Furthermore, the performance of the Pt-Pt O_2 device differs little from previous sensocompatibility studies performed by different groups on different sensors [50,53,54]. More specifically, the lack of any significant difference recorded across the actual homogenate exposure days (Day 1–Day 14) signifies a negligible effect of physiological conditions on the sensor's performance. Collectively, these sensocompatibility results support the ability of the Pt-Pt configuration to provide reliable and stable O_2 readings in physiological tissue with a minimal contribution, if any, from signal drifts.

A final consideration is the well-established dependence of O_2 sensors, including Clark type electrodes and their miniaturised counterparts, on temperature changes *in vivo*. An estimated deviation of *ca.* 3% per 1 °C for Pt electrodes has been reported previously, though this has a negligible impact on brain level recordings due to the highly regulated cerebral temperature levels [28]. However, temperature changes associated with skeletal tissue ischaemia are expected to be much larger and could potentially interfere with O_2 measurements unless compensated for through concurrent temperature monitoring. Since our principle objective was to demonstrate feasibility of the Pt-Pt configuration at measuring O_2 changes during acute ischaemia, the effect of temperature on our O_2 signal was deemed negligible. The temperature effect of a 10-min ischaemic insult under tourniquet control in a porcine model was recorded as < 1 °C, but the temperature decreased linearly over a subsequent three-hour period with an approximate change of *ca.* 10 °C [10], which would have a significant impact on the O_2 signal unless compensated for. This is an important consideration when deploying this Pt-Pt configuration in future models of extremity vascular injury,

ischaemia-reperfusion injury, or locomotion recovery. The next step for this Pt-Pt O$_2$ configuration would be to prove the concept in a human clinical study.

5. Conclusion

We have described the *in vitro* development and *in vivo* validation of a novel Pt-based electrochemical device that permits the continuous real-time measurement of peripheral tissue O$_2$. *In vitro* investigations determined a significant difference in sensitivities recorded for the previously reported Pt-SCE design and our novel Pt configuration at −0.65 V *vs.* reference electrode. Increasing the reduction potential of our Pt design to −0.80 V *vs.* Pt resulted in a significant improvement in sensitivity that was comparable to the Pt-SCE design. The novel ClinOX device demonstrated a good linear sensitivity value over the conventional 0–1200 μM O$_2$ calibration range with the added benefit of being constructed from biocompatible materials that render it suitable for clinical use. The *in vivo* application of both Pt-Pt configurations in the hind limb of anaesthetised rats resulted in significant decreases in O$_2$ currents compared to baseline levels over the course of a 10-min ischaemic insult. Discrepancies in reperfusion characteristics were reported and attributed to the difference in size and geometries of both designs in the rodent model. Subsequently, the ClinOX design was deployed in a porcine model of limb ischaemia and a significant decrease in O$_2$ currents compared to baseline levels was reported. The return of the O$_2$ current to pre-insult levels during reperfusion supports the ability of the ClinOX design to measure real-time O$_2$ perturbations during a period of ischaemia in an animal model that closely represents the size and haemodynamics of the human vascular system. The work described within is a prerequisite for the future deployment of this Pt-Pt ClinOX design in a clinical study of the real-time measurement of O$_2$ levels during tissue ischaemia.

Acknowledgments

Conflict of interests

The authors have no conflict of interest to report.

Author contributions

NJF carried out *in vitro*, *in vivo*, and *ex vivo* experiments and compiled the article. FBB carried out *in vivo* experiments, designed the ClinOX device, and critically reviewed the article.

Appendix A. Supplementary data

Supplementary data to this article can be found online at https://doi.org/10.1016/j.bioelechem.2017.09.010.

References

[1] K.K. Tremper, S.J. Barker, Advances in oxygen monitoring, Int. Anesthesiol. Clin. 25 (1987) R15–R16.

[2] K.K. Tremper, T.W. Rutter, J.A. Wahr, Monitoring oxygenation, Curr. Anaesth. Crit. Care 4 (1993) 213–222.

[3] J.W. Severinghaus, Takuo Aoyagi: discovery of pulse oximetry, Anesth. Analg. 105 (2007) S1–S4.

[4] K.K. Tremper, S.J. Barker, Pulse oximetry, Anesthesiology 70 (1989) 98–108.

[5] M. von Bergh, C. Madler, Tissue Oxygen Saturation in the Emergency and Critical Care SettingEmergency Medicine and Critical Care 2008.

[6] M. Frink, F. Hildebrand, C. Krettek, J. Brand, S. Hankemeier, Compartment syndrome of the lower leg and foot, Clin. Orthop. Relat. Res. 468 (2010) 940–950.

[7] H. Hayakawa, D.J. Aldington, M. A.M., Acute traumatic compartment syndrome: a systematic review of results of fasciotomy, Trauma 11 (2009) 5–35.

[8] C. Jager, V. Echtermeyer, Compartment syndrome of the lower leg and foot. Anatomy and pathophysiology, Unfallchirurg 111 (2008) 768–+.

[9] A. Tiwari, A.I. Haq, F. Myint, G. Hamilton, Acute compartment syndromes, Br J Surg 89 (2002) 397–412.

[10] J.S. Radowsky, J.D. Caruso, R. Luthra, M.J. Bradley, E.A. Elster, J.A. Forsberg, N.J. Crane, Noninvasive multimodal imaging to predict recovery of locomotion after extended limb ischemia, PLoS One 10 (2015).

[11] C. Ince, The microcirculation is the motor of sepsis, Crit. Care 9 (2005) S13–S19.

[12] A. Caselli, D.S. Bedi, C. O'Connor, C. Shah, A. Veves, Assessment of laser Doppler perfusion imager's in vivo reliability: can it be used for a prospective analysis? J. Laser Appl. 14 (2002) 198–202.

[13] M. Roustit, J.L. Cracowski, Non-invasive assessment of skin microvascular function in humans: an insight into methods, Microcirculation 19 (2012) 47–64.

[14] B.A. Crookes, S.M. Cohn, E.A. Burton, J. Nelson, K.G. Proctor, Noninvasive muscle oxygenation to guide fluid resuscitation after traumatic shock, Surgery 135 (2004) 662–670.

[15] K.K. McCully, T. Hamaoka, Near-infrared spectroscopy: what can it tell us about oxygen saturation in skeletal muscle, Exerc. Sport Sci. Rev. 28 (2000) 123–127.

[16] F. Moore, S.M. Cohn, A.B. Nathens, P. Rhee, J.C. Puyana, E.E. Moore, Tissue oxygen saturation predicts the development of organ failure during traumatic shock resuscitation, Inflamm. Res. 56 (2007) S217–S218.

[17] T.W.L. Scheeren, P. Schober, L.A. Schwarte, Monitoring tissue oxygenation by near infrared spectroscopy (NIRS): background and current applications, J. Clin. Monit. Comput. 26 (2012) 279–287.

[18] K.G.B. Elliott, A.J. Johnstone, Diagnosing acute compartment syndrome, J. Bone Joint Surg.Br. Vol. 85B (2003) 625–632.

[19] L.C. Clark, J.A. Helmsworth, S. Kaplan, R.T. Sherman, Z. Taylor, Polarograhpic measurement of oxygen tension in whole blood and tissues during total by-pass of the heart, Surg. Forum 4 (1953) 93–96.

[20] L.C. Clark, R. Wolf, D. Granger, Z. Taylor, Continuous recording of blood oxygen tensions by polarography, J. Appl. Physiol. 6 (1953) 189–193.

[21] A. Ledo, C.F. Lourenco, J. Laranjinha, C.M.A. Brett, G.A. Gerhardt, R.M. Barbosa, Ceramic-based multisite platinum microelectrode arrays: morphological characteristics and electrochemical performance for extracellular oxygen measurements in brain tissue, Anal. Chem. 89 (2017) 1674–1683.

[22] J. Dengler, C. Frenzel, P. Vajkoczy, S. Wolf, P. Horn, Cerebral tissue oxygenation measured by two different probes: challenges and interpretation, Intensive Care Med. 37 (2011) 1809–1815.

[23] W. van Der Brink, A.R. Moos, Brain oxygen tension in severe head injury, Neurosurgery 46 (2000) 868–878.

[24] D.G. Ikossi, M.M. Knudson, D.J. Morabito, M.J. Cohen, J.J. Wan, L. Khaw, C.J. Stewart, C. Hemphill, G.T. Manley, Continuous muscle oxygenation in critically injured patients: a prospective observational study, J. Trauma 61 (2006) 780–788.

[25] E.N. Hansen, G. Manzano, U. Kandemir, J.M. Mok, Comparison of tissue oxygenation and compartment pressure following tibia fracture, Injury 44 (2013) 1076–1080.

[26] J.W. Weick, H. Kang, L. Lee, J. Kuether, X.H. Liu, E.N. Hansen, U. Kandemir, M.D. Rollins, J.M. Mok, Direct measurement of tissue oxygenation as a method of diagnosis of acute compartment syndrome, J. Orthop. Trauma 30 (2016) 585–591.

[27] J.M. Mok, E.N. Hansen, H. Kang, U. Kandemir, Diagnosis of acute compartment syndrome: direct measurement of tissue oxygenation, Tech. Orthop. 27 (2012) 22–29.

[28] F.B. Bolger, R. Bennett, J.P. Lowry, An in vitro characterisation comparing carbon paste and Pt microelectrodes for real-time detection of brain tissue oxygen, Analyst 136 (2011) 4028–4035.

[29] C.D. Johnson, D.W. Paul, In situ calibrated oxygen electrode, Sensors Actuators B Chem. 105 (2005) 322–328.

[30] N. Holmstrom, P. Nilsson, J. Carlsten, S. Bowald, Long-term in vivo experience of an electrochemical sensor using the potential step technique for measurement of mixed venous oxygen pressure, Biosens. Bioelectron. 13 (1998) 1287–1295.

[31] B.J. Venton, D.J. Michael, R.M. Wightman, Correlation of local changes in extracellular oxygen and pH that accompany dopaminergic terminal activity in the rat caudate-putamen, J. Neurochem. 84 (2003) 373–381.

[32] J.B. Zimmerman, R.T. Kennedy, R.M. Wightman, Evoked neuronal activity accompanied by transmitter release increases oxygen concentration in rat striatum in vivo but not in vitro, J. Cereb. Blood Flow Metab. 12 (1992) 629–637.

[33] F.B. Bolger, S.B. McHugh, R. Bennett, J. Li, K. Ishiwari, J. Francois, M.W. Conway, G. Gilmour, D.M. Bannerman, M. Fillenz, M. Tricklebank, J.P. Lowry, Characterisation of carbon paste electrodes for real-time amperometric monitoring of brain tissue oxygen, J. Neurosci. Methods 195 (2011) 135–142.

[34] D.A. Kane, R.D. O'Neill, Major differences in the behaviour of carbon paste and carbon fibre electrodes in a protein-lipid matrix: implications for voltammetry in vivo, Analyst 123 (1998) 2899–2903.

[35] A. Cowley, B. Woodward, A healthy future: platinum in medical applications, Platin. Met. Rev. 55 (2011) 98–107.

[36] X. Liu, M. Zhang, T. Xiao, J. Hao, R. Li, L. Mao, Protein pretreatment of microelectrodes enables in vivo electrochemical measurements with easy precalibration and interference-free from proteins, Anal. Chem. 88 (2016) 7238–7244.

[37] M.M. Patrick, J.M. Grillot, Z.M. Derden, D.W. Paul, Long-term drifts in sensitivity caused by biofouling of an amperometric oxygen sensor, Electroanalysis 29 (2017) 1–9.

[38] B.J. Venton, D.J. Michael, R.M. Wightman, Correlation of local changes in extracellular oxygen and pH that accompany dopaminergic terminal activity in the rat caudate-putamen, J. Neurochem. 84 (2003) 373–381.

[39] G. Inzelt, Pseudo-reference electrodes, in: G. Inzelt, A. Lewenstam, F. Scholz (Eds.), Handbook of Reference Electrodes, Springer, 2013.

[40] N.J. Finnerty, S.L. O'Riordan, F.O. Brown, P.A. Serra, R.D. O'Neill, J.P. Lowry, In vivo characterisation of a Nafion®-modified Pt electrode for real-time nitric oxide monitoring in brain extracellular fluid, Anal. Methods 4 (2012) 550–557.

[41] N.J. Finnerty, S.L. O'Riordan, E. Palsson, J.P. Lowry, Brain nitric oxide: regional characterisation of a real-time microelectrochemical sensor, J. Neurosci. Methods 209 (2012) 13–21.

[42] N. Finnerty, S. O'Riordan, D. Klamer, J. Lowry, E. Palsson, Increased brain nitric oxide levels following ethanol administration, Nitric Oxide 47 (2015) 52–57.

[43] C.H. Reid, N.J. Finnerty, Long term amperometric recordings in the brain extracellular fluid of freely moving immunocompromised NOD SCID mice, Sensors 17 (2017) 419–434.

[44] S. Lofti, A.S. Patel, K. Mattock, K. Eggington, A. Smith, B. Modarai, Towards a more relevant hind limb model of muscle ischaemia, Atherosclerosis 227 (2013) 1–8.

[45] R. Paek, D.S. Chang, L.S. Brevetti, M.D. Rollins, S. Brady, P.C. Ursell, T.K. Hunt, R. Sarkar, L.M. Messina, Correlation of a simple direct measurement of muscle pO2 to a clinical ischemia index and histology in a rat model of…, J. Vasc. Surg. 36 (2002) 172–179.

[46] A.A. Hellingman, A.J.N.M. Bastiaansen, M.R. de Vries, L. Seghers, M.A. Lijkwan, C.W. Lowik, J.F. Hamming, P.H.A. Quax, Variations in surgical procedures for hind limb ischaemia mouse models result in differences in collateral formation, Eur. J. Vasc. Endovasc. Surg. 40 (2010) 796–803.

[47] T. Couffinhal, M. Silver, L.P. Zheng, M. Kearney, B. Witzenbichler, J.M. Isner, Mouse model of angiogenesis, Am. J. Pathol. 152 (1998) 1667–1679.

[48] G. Bosco, Z. Yang, J. Nandi, J. Wang, C. C., E.M. Camporesi, Effects of hyperbaric oxygen on glucose, lactate, glycerol and anti-oxidant enzymes in the skeletal muscle of rats during ischaemia and reperfusion, Clin. Exp. Pharmacol. Physiol. 34 (2007) 70–76.

[49] J.P. Lowry, M.G. Boutelle, M. Fillenz, Measurement of brain tissue oxygen at a carbon past electrode can serve as an index of increases in regional cerebral blood flow, J. Neurosci. Methods 71 (1997) 177–182.

[50] N. Wisniewski, F. Moussy, W.M. Reichert, Characterization of implantable biosensor membrane biofouling, Fresenius J. Anal. Chem. 366 (2000) 611–621.

[51] A.M. Wynne, C.H. Reid, N.J. Finnerty, In vitro characterisation of ortho phenylenediamine and Nafion-modified Pt electrodes for measuring brain nitric oxide, J. Electroanal. Chem. 732 (2014) 110–116.

[52] C.P. Pennisi, C. Sevcencu, A. Dolatshahi-Pirouz, M. Foss, J.L. Hansen, A.N. Larsen, V. Zachar, F. Besenbacher, K. Yoshida, Responses of fibroblasts and glial cells to nano-structured platinum surfaces, Nanotechnology 20 (2009).

[53] A. Weltin, J. Kieninger, G.A. Urban, Microfabricated, amperometric, enzyme-based biosensors for in vivo applications, Anal. Bioanal. Chem. 408 (2016) 4503–4521.

[54] R. Gifford, J.J. Kehoe, S.L. Barnes, B.A. Kornilayev, M.A. Alterman, G.S. Wilson, Protein interactions with subcutaneously implanted biosensors, Biomaterials 27 (2006) 2587–2598.